Accurate and Efficient Separation of Left and Right Lungs from 3D CT Scans: a Generic Hysteresis Approach

Ziyue Xu, Ulas Bagci*, Colleen Jonsson, Sanjay Jain, and Daniel J. Mollura

***Abstract*— Separation of left and right lungs from binary segmentation is often necessary for quantitative image-based pulmonary disease evaluation. In this article, we present a new fully automated approach for accurate, robust, and efficient lung separation using 3-D CT scans. Our method follows a hysteresis setting that utilizes information from both lung regions and background gaps. First, original segmentation is separated by subtracting the gaps between left and right lungs, which are enhanced with Hessian filtering. Second, the 2-D separation manifold in 3-D image space is estimated based on the distance information from the two subsets. Finally, the separation manifold is projected back to the original segmentation in order to produce the separated lungs through optimization for addressing minor local variations. An evaluation on over 400 human and 100 small animal 3-D CT images with various abnormalities is performed. The proposed scheme successfully separated all connections on the candidate CT images. Using hysteresis mechanism, each phase is performed robustly and 3-D information is utilized to achieve a generic, efficient, and accurate solution.**

***Index Terms*— Left and right lung separation, hysteresis, Hessian, distance transform, lung segmentation**

I. Introduction

Chest CT images provide important information for quantification of pulmonary diseases. In routine clinics, quantification is often done manually. Therefore, computer aided diagnostics (CAD) targeting at analysis of lung anatomy have been an active research area to rase this manual task.The aim in CAD system is to provide efficient and robust solutions to process large data sets and improve accuracy. Among various CAD methods, lung segmentation is the most commonly applied to define the lung region as a precursor step for further assessments. Moreover, as a final step of lung segmentation, morphological operations are often utilized to smooth lung boundaries that can be locally distorted by segmentation methods. However, since the gap at anterior and posterior junctions between left and right lungs can be very small, such operation can cause the two lung regions to fuse with each other. Meanwhile, it is necessary for accurate lung function evaluation to measure left and right lungs individually. Consequently, an efficient and accurate algorithm for separating two lungs is needed.

In spite of the demand for a generic solution, the details of the lung separation algorithms is often limited in the literature. The challenges for this task is caused by large variations for lung anatomies, pathologies, and fusion areas. As shown in Fig. 1, irregular shape of lungs can violate the assumption regarding lung locations in the image (A), pathologies can cause large intensity variations and local multi-separations (B), and fusion areas can be wide with low contrast for certain subjects (C).

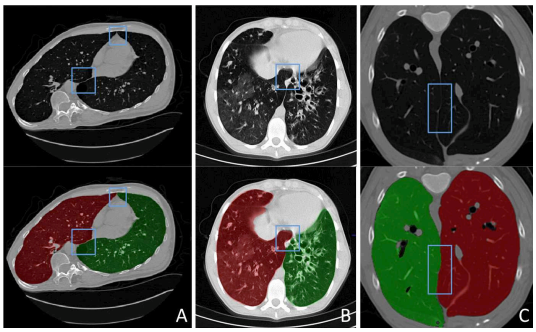

Fig. 1. Challenges for left and right lung separation: irregular shape (A), intensity variation caused by pathologies (B), and low contrast wide fusion (C).

Conventionally, most methods focus on 2-D slice-wise operations using information from either lung regions or gap locations. For applications without accuracy requirement, this task can be as simple as cutting through the slice middle line [1]. Morphological operations can also be applied to the binary lung mask to figure out the thinnest joint [2]. This method is based on the lung region shape information. However, the kernel size is needed to be different for different cases and there is no guarantee that the resulting location aligns with the true gap. Further, region growing algorithms from two seeds [3] could capture the "collision" when two growing process meet each other. This method utilizes the intensity information of the lung regions, whereas the process needs to be carefully designed to ensure growth in left and right lungs meet each other at the correct location. This is crucial especially for cases with disease where the intensity variation is large. The state-of-the-art and most commonly applied methods are based on minimum path [4]–[6] strategies. These methods are performed on 2-D slices and focus on the gap regions instead of candidate lung itself. They usually identify suspicious area of connection first, and then search for the accurate separating line/curve between the two lungs using dynamic programming. It has been shown that they can accurately estimate the separation, however, the method is limited in several aspects. The detection of connecting areas may not be always accurate, and multiple

*This research is supported by CIDI, the intramural research program of the National Institute of Allergy and Infectious Diseases (NIAID) and the National Institute of Biomedical Imaging and Bioengineering (NIBIB).

Z. Xu, U. Bagci, and D. J. Mollura are with Center for Infectious Disease Imaging, Radiology and Imaging Sciences, National Institutes of Health, Bethesda, MD; C. Jonsson is with University of Louisville, Louisville, KY; S. Jain is with Johns Hopkins University, Baltimore, MD.

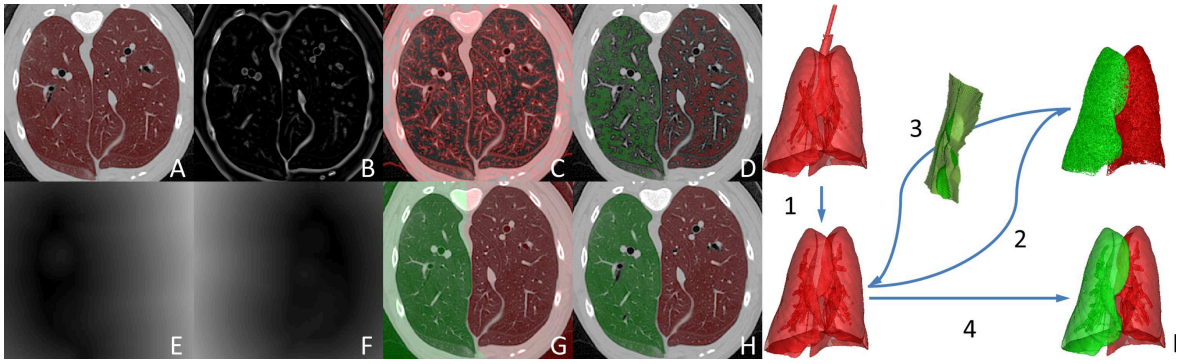

Fig. 2. Flow chart of the proposed algorithm. (A) Original CT image with binary lung segmentation, (B) Hessian analysis enhancing bright plate-like structures, (C) enhanced plate structure, (D) point groups from separated left and right lung regions by subtracting the dilated plate structures from original segmentation, (E, F) distance transform from the two point groups, (G) 2-D separation manifold determined by distance transform, (H) final separation result, and (I) illustration of the general hysteresis setting.

"optimal" paths can present in the connecting areas. For detection, iterative morphological operation is often performed and compared with the original segmentation. Thus it is both time consuming and inaccurate to identify the correct connection locations. For "optimal" path identification, due to the fact that the method is confined within 2-D slice plane, dynamic programming may create false optimal path along the bright lung area formed by lung structure appearance, vessel, and/or pathologies. Hence, the optimality of resulting separation is local and can be compromised under many circumstances. 3-D information between slices can be incorporated to improve the performance by reinforcing additional constraints over the location of start/end points, but it adds limited information and is computationally expensive. Also, the robustness is limited since errors are propagated along the sequential operations. More recently, 3-D active shape model methods are proposed [7], [8] and model is generated for left and right lungs separately. Although, left and right lungs are estimated independently and there is no need to explicitly perform lung separation, it fails to provide a generic solution for other lung segmentation methods.

In this study, we propose a new method to address the challenges of the lung separation task and avoid the drawbacks of the state-of-the-art methods. As shown in Fig. 2 (I), the algorithm follows a hysteresis setting that utilizes full 3-D information from both lung regions and background gaps. Without loss of generality, we use the conventional region growing method for initial lung segmentation. Other more advanced methods can also be applied. Note that the results by region grow usually include trachea regions, thus Step 1 in Fig. 2 (I) is to remove the trachea from the whole lung segmentation, resulting in the 3-D lung volume without trachea (Fig. 2 (A)). Then, in Step 2, bright plate-like structures in the original image is enhanced by Hessian filtering (Fig. 2 (B)), and the extracted plate structures (Fig. 2 (C)) are subtracted from the original lung segmentation. By applying connected component analysis, voxel groups belonging to left and right lungs can be separately labeled (Fig. 2 (D)). In Step 3, distance transform from the two groups are calculated (Fig. 2 (E, F)), and the 2-D separation manifold in 3-D image space is estimated based on the distances (Fig. 2 (G)). Lastly, in Step 4, the separation manifold is projected back to the original segmentation result and local optimization is performed to generate the final separated left and right lung regions. By following hysteresis design and using 3-D information from both lungs and gap regions, the presented method eliminated the need for connection region detection and the separation manifold can be estimated regardless of connection number, location, length, and local intensity variations. Also, the estimation is done according to 3-D information instead of slice-by-slice manner, thus it avoids local variations and captures the separation efficiently. In the next section, the proposed framework is presented in detail.

II. Theory and Algorithms

In this section, we first briefly introduce the initial lung segmentation method based on the theory of fuzzy connectedness (FC) [9] image segmentation along with trachea detection [10]. Subsequently, plate-like structure enhancement is explained following the Hessian filtering [11]. Finally, the theory and algorithm of a new lung separation approach is formulated that combines the methods to accurately estimate the separating manifold.

A. Lung and Trachea Segmentation

A computer-aided detection scheme is applied to CT images for seed point generation of trachea regions. Specifically, adaptive threshold and connected component analysis is first utilized to extract shape features of the regions of interest. Then, a supervised machine learning method of support vector machine is applied to detect trachea [10] with accuracy of more than 99%. After detection, lung and trachea regions are extracted using FC with the detected seed points.

FC determines the closeness of any two voxels p and q in the image space, using information along pathes $\pi \in \mathcal{P}(p,q)$ between them, while π denotes a certain path consists of a sequence of voxels $\langle p_0 = p, p_1, p_2, ..., p_N = q \rangle$ such that voxel p_i and p_{i+1} are adjacent to each other, $\mathcal{P}(p,q)$ denotes the set of all paths between p, q. For adjacent voxels, an affinity function $\mu_\kappa(p_i, p_{i+1})$ can be defined based on

their intensity similarity. Then, the strength of path π is determined by the weakest link along the path

$$\mu_{\mathcal{N}}(\pi) = \min_{1 \le i < N} \mu_{\kappa}(p_i, p_{i+1}). \quad (1)$$

Further, FC between two voxels p, q is the strength of the strongest path,

$$\mu_K(p, q) = \max_{\pi \in \mathcal{P}(p,q)} \mu_{\mathcal{N}}(\pi). \quad (2)$$

In this way, a fuzzy relationship $\mathcal{O}$ can be calculated for every voxel in an image from a predetermined set of seeds S as

$$\mu_{\mathcal{O}}(p) = \max_{s \in S} \mu_K(p, s), \quad (3)$$

simulating a region grow process. Finally, segmentation of target object can be achieved with threshold. Herein, we use two threshold levels over the same FC map for segmenting trachea and lung simultaneously.

B. Plate Structure Enhancement

In 3-D pulmonary CT images, the boundary of lung regions, especially the connection region between the two lungs, can be regarded as bright plate-like structures on the dark background. Identification and delineation of such structures can be improved by enhancement algorithms. As shown in [11], analyzing the second-order information (Hessian) of a Gaussian convoluted image provides local information of the structure. Specifically, eigenvalue decomposition is performed over the Hessian matrix and the resulting ordered eigenvalues, i.e., $(|\lambda_1| \le |\lambda_2| \le |\lambda_3|)$, are examined. For voxels within bright plate-like structures in particular, it is expected that both λ_1 and λ_2 are small while λ_3 is large and negative. Explicitly, the plateness can be formulated as

$$P_\sigma = \begin{cases} 0, & \text{if } \lambda_3 > 0; \\ e^{-\frac{R_B^2}{2\beta^2}}(1 - e^{-\frac{S^2}{2\gamma^2}}), & \text{otherwise,} \end{cases} \quad (4)$$

where $R_B = |\lambda_2|/|\lambda_3|$, and $S = \sqrt{\lambda_1^2 + \lambda_2^2 + \lambda_3^2}$. The plateness measure above is calculated at different scales (σ) and the maximum response will be achieved at a scale that matches the size of the plate. Therefore, by using a multi-scale approach which covers a range of widths and finding the maximum value $V = \max(V_\sigma), \sigma_{\min} \le \sigma \le \sigma_{\max}$, we get the plateness measure for each voxel in the image.

C. Hysteresis Lung Separation

After removing trachea from the whole lung segmentation and enhancing all plate-like gaps, we design a hysteresis lung separation scheme. First, in order to separate the points of lung segmentation into left and right regions, our aim is to keep the approximate shape of each one as much as possible. Hence, iterative morphological operation is not feasible for this task since the detailed shape information is lost during the erosion process. Notice that the inside of each lung does not to be preserved perfectly since it is not necessary to keep all points inside each lung when determine left/right affiliation. Therefore, we make use of the plateness computation to ensure separation of each lung while keep the approximate shape information. As illustrated in Fig. 2 (B), plate structures are enhanced so that the gap between two lungs are captured with liberal threshold and expanded with morphological dilation, resulting in liberal Fig. 2 (C). As shown, we then "over-subtract" the tissues from lung regions, which ensures that the remaining tissues can be separated in to left and right lungs by connected component analysis in Fig. 2 (D), and this completes the forward phase of hysteresis as shown in Fig. 2 (I.2). Next, the separation manifold in 3-D image space is estimated using these two data point sets S_{L} and S_{R}. Here, we used the 3-D Euclidean distance transform (DT) to estimate the range to each individual lungs as shown in Fig. 2 (E, F). As shown in Fig. 2 (I), since the shape information is preserved from the forward phase, the separation manifold Fig. 2 (G) can be efficiently estimated satisfying $DT(S_{\mathrm{L}}) \approx DT(S_{\mathrm{R}})$. The separation manifold is projected back into the original segmentation in order to separate the left and right lungs, and this completes the backward phase of hysteresis (Fig. 2 (I.3)). Last, to account for minor local variations, regions within small distance (e.g. 5 voxels) on either side of the estimated manifold is marked "fuzzy", and their labels are further refined by the spatial relationship to the confident regions via FC (Fig. 2 (H, I.4)). The last step is optional, and from our observation, the estimated separation performs well for most cases. Indeed, the additional refinement step is helpful for difficult circumstances.

In this way, the searching process for detection of the connection, which can lead to significant error, is avoided. Also, full 3-D information is utilized, so that the optimal separating manifold is generated in a single pass, instead of searching for the optimal path in every slice and propagate to the next slice, which lead to sub- and local-optimality.

III. Results

To evaluate the performance of our lung separation method, we used both human and small animal data sets. A large data set consisting of over 400 human and 100 small animal 3-D CT images with various abnormalities is performed. Images were acquired using 64-detector row Phillips Brilliance 64 or GE Medical Systems Light Speed Ultra. Scans were performed at end-inspiration with 1.0 or 2.0 collimation and obtained at 10 or 20 mm intervals from the base of the neck to upper abdomen. Slice thickness ranges from 0.8 mm to 5 mm, while in-plane resolution ranges from 0.5×0.5 mm to 0.8×0.8 mm. For small animal images (rabbits and ferrets), the spatial resolution range from 0.2×0.2 mm to 0.3×0.3 mm in plane and 0.2 mm to 0.6 mm between slices ([10], [12]).

In the context of segmentation, the "gold standard" is usually not available. Instead, manual delineation is often used as reference standard. However, for left and right lung separation, as it appears a 2-D separation manifold in 3-D space, it is extremely tedious and time consuming for human to define the border of two lungs by tracing the voxels visually brighter than neighboring lung tissues for the entire

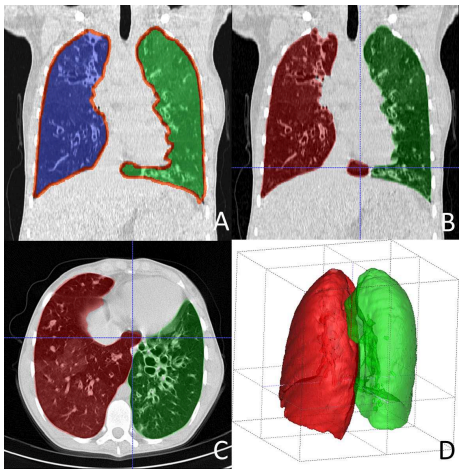

Fig. 3. Result compared with Reference segmentation from LOLA Challenge (A) Separation given by LOLA reference. (B) Separation produced by the proposed method. (C) Corresponding axial view confirming the observation that the part of right lung is mistakenly included in the left in reference LOLA image, which is corrected by the proposed method. (D) 3-D rendering of the separated lungs

3-D image. Here, we first performed a visual qualitative evaluation of all images by two experts for the performance of the proposed separation algorithm. The results are categorized to "successful" if there is no significant error for separation with only minor zigzag boundary variations, and "unsuccessful" if a part of the lung is falsely separated. The observation is performed on all three orientations in order to avoid false judgements. Fig. 3 shows an example of "unsuccessful" false separation produced by other methods from LOLA challenge data (*http://lola11.com*) in (A). The figure shows a reference ground truth and our method's separation in (B) such that the area centered at the cross is falsely included in the wrong lung (i.e., left lung were falsely labeled as right lung) while the same region was correctly labeled with proposed algorithm. Fig. 3(C) confirmed the observation from axial view, and (D) provides a 3-D rendering for the separation result. This example illustrates the importance of using 3-D information instead of 2-D information that can potentially introduce bias to the final result. For testing dataset, the proposed algorithm successfully separated all connections on the candidate CT images efficiently with proper parameters. Our study shows that with default parameters, all human images can be successfully processed, whereas tuning is needed for 5% of small animal images.

Beyond qualitative evaluation, 100 slices of connection samples are collected covering object, resolution, and appearance variations. Experts are asked to manually draw the separation curves between the left and right lungs on the overlapping segmentation mask, and Hausdorff distance (HD) is computed between the result from proposed method and the reference. The experimental results showed that by applying the 3-D hysteresis method, left and right lungs for all testing cases are successfully separated, and the average HD is 0.4 pixels. The whole computation time including plateness and distance transform is 3 minutes for an image with size $512 \times 512 \times 658$ on a 3.7 GHz machine running Linux system.

IV. Conclusion

CAD systems has been proved helpful for radiologists in diagnosing lung diseases. Lung segmentation is an important component for many CAD tasks. As the last step of lung segmentation, separation of left and right lungs is an essential procedure, since it enables more specific and accurate quantification of local lung functions. Conventional methods conducting separation in 2-D slice plane with potential connection detection and shortest path computation, hence suffer from limited accuracy and robustness. To address the challenges due to various connection situations, in this paper, we proposed a new full 3-D lung separation method using a hysteresis setting in defining the separation manifold within 3-D image space. The proposed method holds no assumption for the potential connection locations, therefore, it is capable to handling different cases of lung segmentation. The scheme combines plateness computation and distance transform to robustly estimation the range of the two individual lungs. As it avoids the complex searching process and utilizes 3-D information, the proposed method outperforms state-of-the-art methods in robustness, accuracy, and efficiency.

References

[1] J. Heuberger, A. Geissbuhler, and H. Muller, "Lung CT segmentation for image retrieval using the insight tookit(ITK)," in *MIT 2005*, 2005.

[2] J.S. Silva, A. Silva, and B.S. Santos, "Lung segmentation methods in X-ray CT images," in *SIARP 2000*, 2000.

[3] R. Shojaii, J. Alirezaie, and P. Babyn, "Automatic lung segmentation in ct images using watershed transform," in *ICIP 2005*, Sept 2005, vol. 2, pp. II–1270–3.

[4] M.S. Brown, M.F. McNitt-Gray, N.J. Mankovich, J.G. Goldin, J. Hiller, L.S. Wilson, and D.R. Aberie, "Method for segmenting chest CT image data using an anatomical model: preliminary results," *Medical Imaging, IEEE Trans.*, vol. 16, no. 6, pp. 828–839, Dec 1997.

[5] S. Hu, E.A. Hoffman, and J.M. Reinhardt, "Automatic lung segmentation for accurate quantitation of volumetric X-ray CT images," *Medical Imaging, IEEE Trans.*, vol. 20, no. 6, pp. 490–498, June 2001.

[6] S.C. Park, J.K. Leader, J. Tan, G.S. Lee, S.H. Kim, I.S. Na, and B. Zheng, "Separation of left and right lungs using 3-dimensional information of sequential computed tomography images and a guided dynamic programming algorithm," *Journal of Computer Assisted Tomography*, vol. 35, no. 2, 2011.

[7] S. Sun, C. Bauer, and R. Beichel, "Automated 3-d segmentation of lungs with lung cancer in ct data using a novel robust active shape model approach," *Medical Imaging, IEEE Trans.*, vol. 31, no. 2, pp. 449–460, Feb 2012.

[8] M. Sofka, J. Wetzl, N. Birkbeck, J. Zhang, T. Kohlberger, J. Kaftan, J. Declerck, and S. Zhou, "Multi-stage learning for robust lung segmentation in challenging ct volumes," in *MICCAI*, vol. 6893 of *Lecture Notes in Computer Science*, pp. 667–674. 2011.

[9] J.K. Udupa and S. Samarasekera, "Fuzzy connectedness and object definition: Theory, algorithms, and applications in image segmentation," *CVGIP: Graph. Model & Imag. Proc.*, vol. 58, no. 3, pp. 246–261, 1996.

[10] Z. Xu, U. Bagci, A. Kubler, B. Luna, S. Jain, W.R. Bishai, and D.J. Mollura, "Computer-aided detection and quantification of cavitary tuberculosis from CT scans," *Medical Physics*, vol. 40, no. 11, 2013.

[11] A. Frangi, W. Niessen, K. Vincken, and M. Viergever, "Multiscale vessel enhancement filtering," in *MICCAI 1998*, 1998, vol. 1496, pp. 130–137.

[12] U. Bagci, B. Foster, K. Miller-Jaster, B. Luna, B. Dey, W. Bishai, C. Jonsson, S. Jain, and D.J. Mollura, "A computational pipeline for quantification of pulmonary infections in small animal models using serial pet-ct imaging," *EJNMMI Research*, vol. 3, no. 1, pp. 55, 2013.